# Influence of anthropogenic aerosol on cloud optical depth and albedo shown by satellite measurements and chemical transport modeling

**Stephen E. Schwartz*[†], Harshvardhan[‡], and Carmen M. Benkovitz***

*Atmospheric Sciences Division, Brookhaven National Laboratory, Upton, NY 11973; and [‡]Department of Earth and Atmospheric Sciences, Purdue University, West Lafayette, IN 47907-1397

Communicated by James E. Hansen, Goddard Institute for Space Studies, New York, NY, December 31, 2001 (received for review June 8, 2001)

## Figure Legends

Figure 1. Sulfate column burden (vertical integral of concentration) in mid North Atlantic at 1800 Universal Time Coordinated (UTC) on April 2-8, 1987 and April 24-29, 1987, as evaluated with a chemical transport and transformation model. Note logarithmic scale. Boxes denote areas chosen for analysis of satellite retrievals of cloud properties.

Figure 2. Time series of sulfate column burden from chemical transport model and pixel-average (1 km × 4 km) cloud properties determined from satellite retrievals over mid North Atlantic, 25-30˚W, 50-55˚N, April 2-8, 1987 (Figure 2.1, left) and 20.25-23.625 ˚W, 43.875-47.25 ˚N, April 24-29, 1987 (Figure 2.2, right). *a*) Modeled sulfate column burden, obtained by interpolation of model output at 6-h intervals; *b*) Effective radius at cloud top, $r_e$; *c*) Optical depth, $\tau_c$; *d*) Cloud-top spherical albedo, $\alpha_{sph}$; *e*) Cloud-top temperature (note inverted scale); *f*) Liquid water path, LWP; *g*) Enhancement of cloud-top spherical albedo relative to that calculated for April 2 (Figure 2.1) or April 24 (Figure 2.2) for the same LWP distribution. Bars denote central 80% of the data; ticks note upper quartile, median, and lower quartile. Two sets of data are shown for April 8, 27, and 28, for which the study area was within range of the satellite on two successive overpasses. Dates and times are UTC.

Figure 3. Pixel-average cloud optical depth $\tau_c$ as a function of vertical cloud liquid water path for eight satellite overpasses over the study area 50-55˚N, 25-30˚W, for April 2-8, 1987. Data points with $\tau_c > 70$ are plotted at $\tau_c = 70$ because of insensitivity of retrieval method at high optical depth; these points are evident as horizontal clusters at $\tau_c = 70$. Data points with $\tau_c \lesssim 3$ have been excluded to eliminate pixels that could be covered by haze but not clouds. Lines denote cloud optical depth for indicated constant values of effective radius near cloud top, $r_e$.

Figure 4. Pixel-average cloud spherical albedo as a function of vertical cloud liquid water path, for three satellite overpasses a) for the first episode, study area 50-55˚N, 25-30˚W, and b) for the second episode, study area 43.875-47.25 ˚N, 20.25-23.625 ˚W, for indicated dates in April, 1987. Clusters of points at albedo ~0.88 represent points with $\tau_c > 70$ for which spherical albedo was calculated as if $\tau_c = 70$. Curves denote cloud albedo for indicated constant values of effective radius near cloud top, $r_e$.

Figure 5. Enhancement of pixel-average cloud spherical albedo $\Delta\alpha_{sph}$ on April 5, 1987, relative to that on April 2, as a function of LWP, for the study area 50-55˚N, 25-30˚W. $\Delta\alpha_{sph}$ was evaluated for each datum of April 5 as the difference between $\alpha_{sph}$ obtained by Eq 2 from $\tau_c$ and $r_e$ obtained from satellite data for that date and the value at the same LWP calculated using a linear fit of $\tau_c$ to LWP for the April 2 data. Data points for $\tau_c > 70$ (592 data out of a total of 6443) were calculated for $\tau_c = 70$ and lie along the diagonal line at the upper right of the cluster of points.

Figure 1

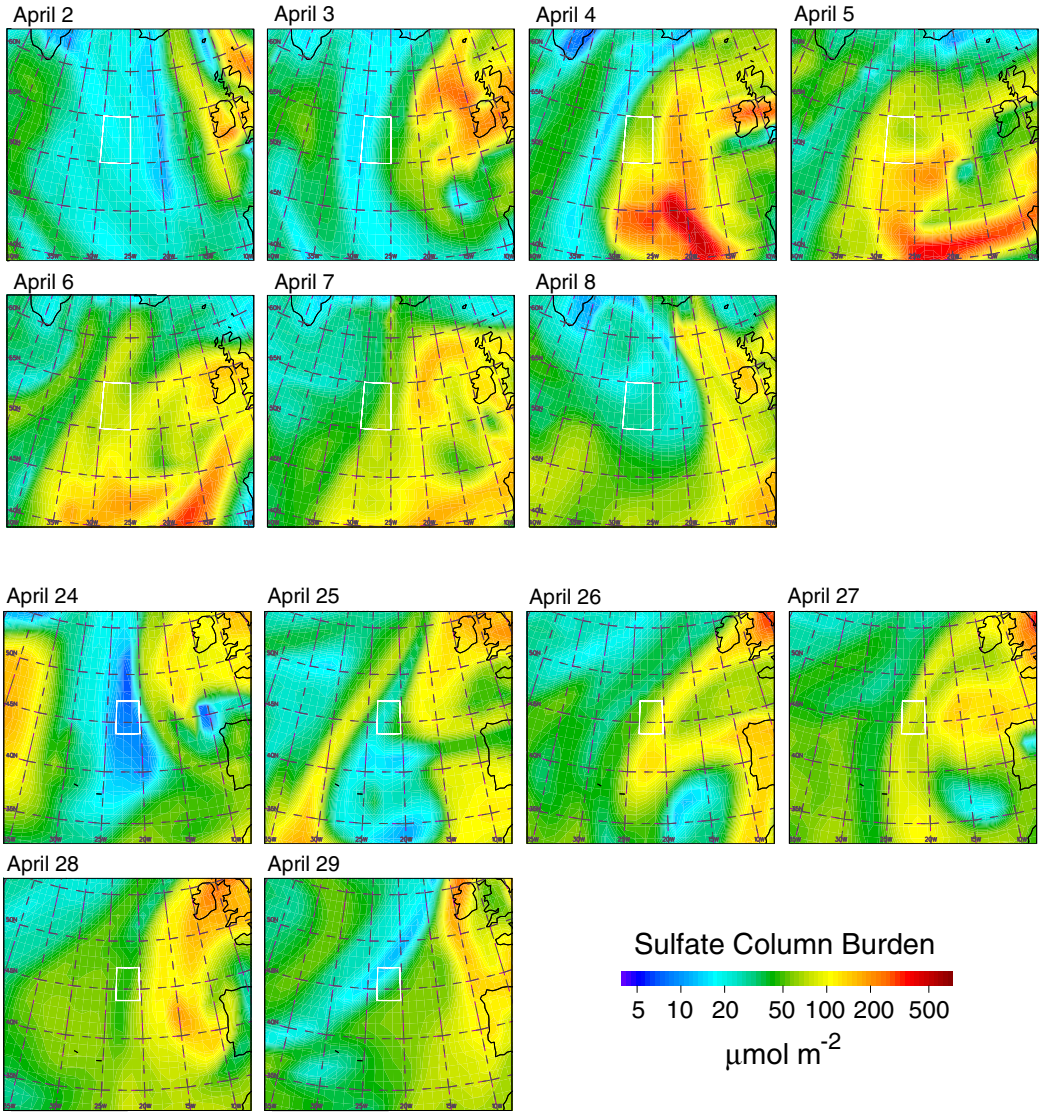
April 2
April 3
April 4
April 5
April 6
April 7
April 8
April 24
April 25
April 26
April 27
April 28
April 29
Sulfate Column Burden
5 10 20 50 100 200 500
µmol m-2

Figure 2

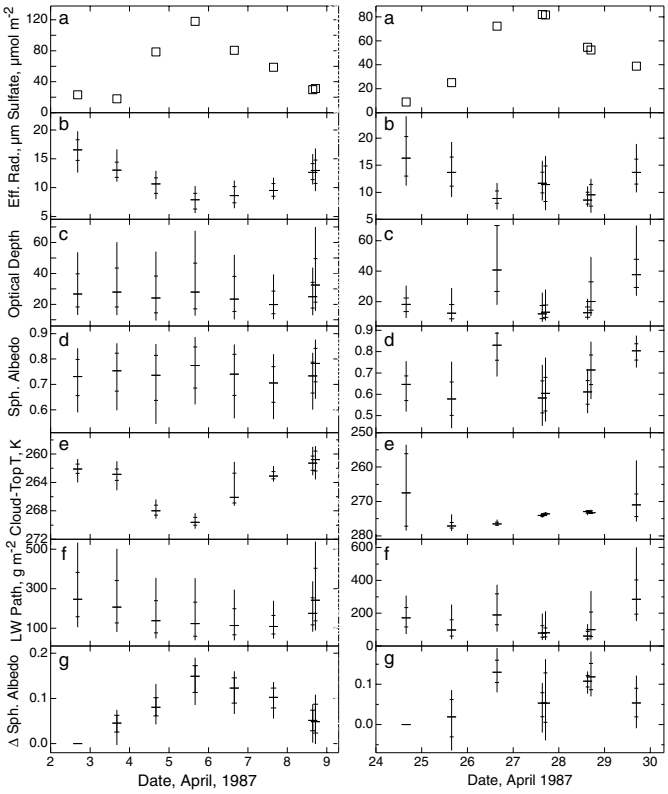
a
b
c
d
e
f
g
Sulfate, μmol m-2
Eff. Rad., μm
Optical Depth
Sph. Albedo
Cloud-Top T, K
LW Path, g m-2
Δ Sph. Albedo
Date, April, 1987
Date, April 1987

Figure 3

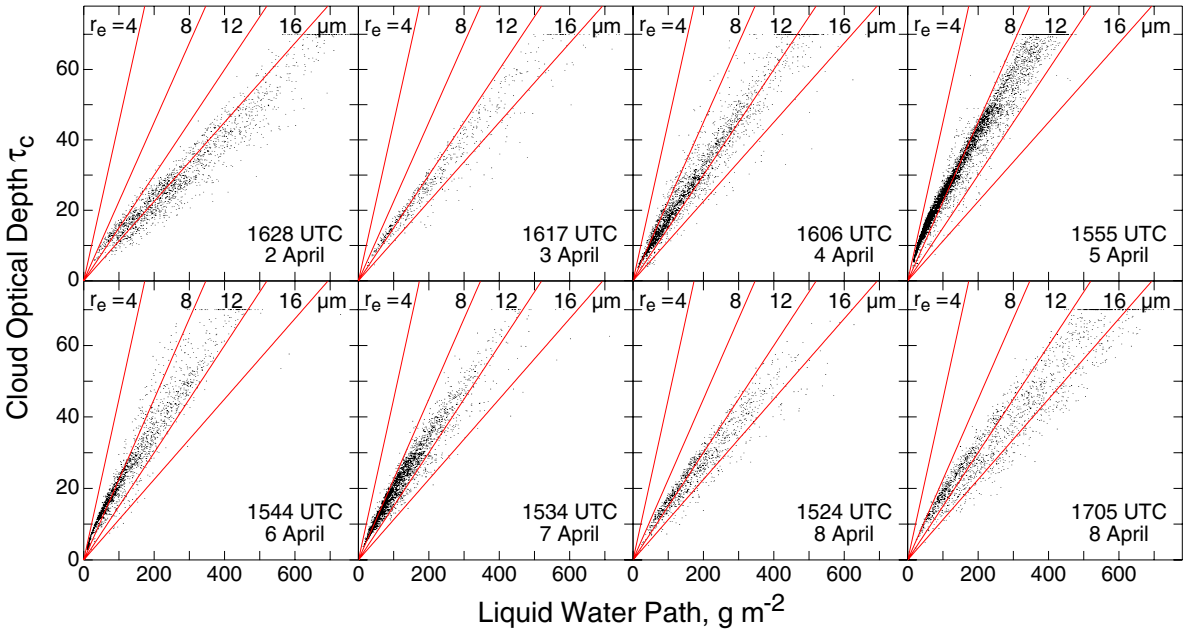
Cloud Optical Depth $\tau_c$
Liquid Water Path, g m$^{-2}$
$r_e$ =4 8 12 16 μm
1628 UTC
2 April
1617 UTC
3 April
1606 UTC
4 April
1555 UTC
5 April
1544 UTC
6 April
1534 UTC
7 April
1524 UTC
8 April
1705 UTC
8 April
0 20 40 60
0 200 400 600

Figure 4

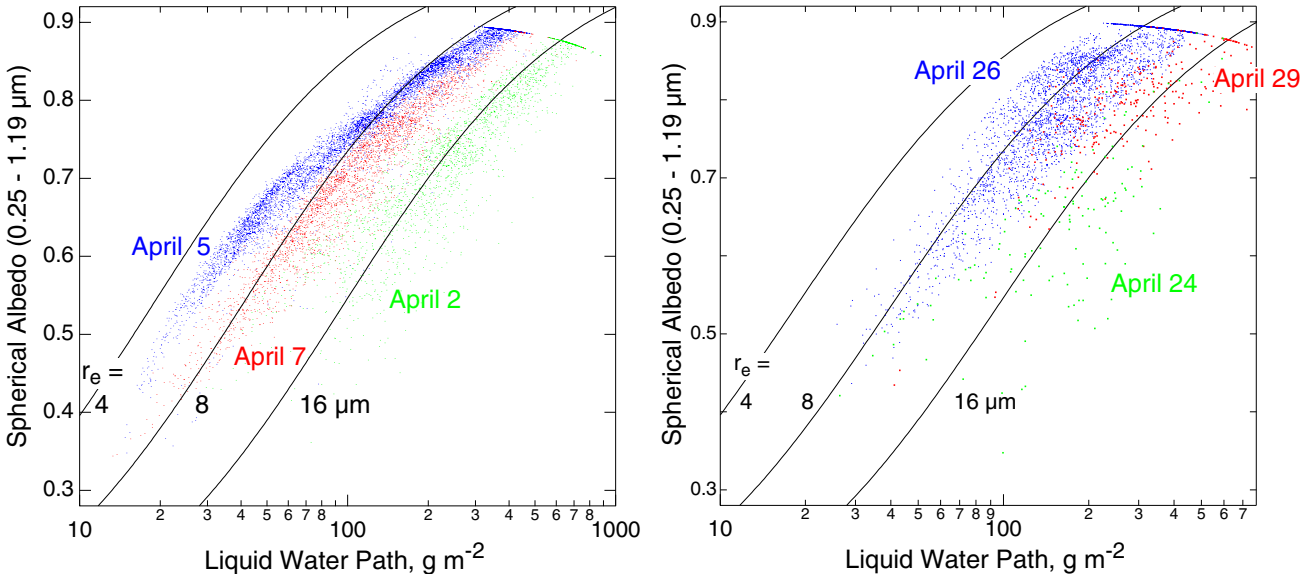
Spherical Albedo (0.25 - 1.19 µm)
Liquid Water Path, g m-2
April 5
April 7
April 2
April 26
April 29
April 24
re =
4
8
16 µm

Figure 5

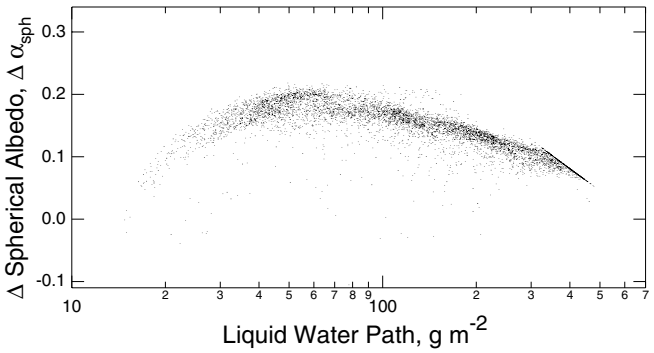
Δ Spherical Albedo, Δ $\alpha_{sph}$
0.3
0.2
0.1
0.0
-0.1
10
2
3
4
5
6
7
8
9
100
2
3
4
5
6
7
Liquid Water Path, g $m^{-2}$